PROGRESS IN COLOR, COLORANTS AND COATINGS

available online @ www.pccc.icrc.ac.ir

Progress in Color Colorants Coating 18 (2025), 177-188

Ministry of Science, Research and Technology
Institute for Color Science & Technology

Optimizing the Surfactant/Polymeric Dispersant Combination in Pigment-Based Aqueous Inkjet Inks

M. Jalili[*1], M. Mohammad Raei Naeini[1], S. Bastani[1,2], N. Ajili[1]**

1 Department of Printing Science and Technology, Institute for Color Science and Technology, P.O. Box: 32465-654, Tehran, Iran.

2 Department of Surface Coating and Corrosion, Institute for Color Science and Technology, P.O. Box: 32465-654, Tehran, Iran.

ARTICLE INFO

Article history:
Received: 27 July 2024
Final Revised: 20 Sept 2024
Accepted: 21 Sept 2024
Available online: 23 Oct 2024

Keywords:
Pigment dispersion
Inkjet printing
Polymeric dispersant
Surfactant
Interface

ABSTRACT

Pigment-based inkjet printing offers numerous advantages over traditional contact printing techniques; however, these inks require stringent dispersion properties and a delicate balance between rheological behavior and surface tension. This study addresses these challenges by exploring and optimizing the combination of surfactants and dispersing agents. We aimed to achieve a stable nanosized dispersion of Disperse Blue 359 in aqueous pigment-based inkjet inks while adjusting its rheological properties using a polymeric dispersant and surfactants. Various formulations with different surfactants and polymeric dispersant concentrations were assessed for rheological behavior, surface tension, particle size distribution, and dispersion stability. Among the assessed surfactants, the surfactant with the lowest hydrophilic-lipophilic balance offered the lowest and most stable particle size. It also showed the best performance during milling and almost Newtonian rheological behavior. It was attributed to its higher tendency to absorb on the particle surface. The optimization of polymeric dispersant concentration also revealed that samples with too low dispersant, experience flocculation rapidly after milling due to insufficient dispersant to cover the fresh surface of ground particles. On the other hand, samples with too high dispersant concentration have stability issues and also non-Newtonian rheological behavior because of too thick absorbed layer of dispersant on the particle surface and high concentration of non-absorbed polymer chains in the media. The optimized combination resulted in a stable nanosized pigment dispersion with low viscosity and Newtonian behavior. These findings provide valuable insights into formulating high-performance pigment-based inkjet inks, highlighting the critical interplay between dispersants and surfactants in achieving optimal performance. Prog. Color Colorants Coat. 18 (2025), 177-188© Institute for Color Science and Technology.

1. Introduction

In recent decades, inkjet printing inks have been under the limelight by various researchers owing to their enormous advantages over traditional printing methods. As a non-contact technique, inkjet printing offers several benefits, including reduced complexity, smaller and less sophisticated printing machines,

*Corresponding author: * Jalili @icrc.ac.ir
** mnnayini@icrc.ac.ir

https://doi.org/10.30509/pccc.2024.167361.1316

no need for pretreatment, and most notably, the absence of stencils or plates. These features confer substantial superiority in terms of customization. Unlike traditional contact printing methods such as offset and gravure, inkjet printing can produce any desired print job, regardless of the print run size, making it highly versatile and efficient for customized and short-run printing tasks. Additionally, inkjet printing generates less waste and has a lower environmental footprint. Collectively, these advantages position inkjet printing robustly in various rapidly growing markets. For instance, the compound annual growth rate (CAGR) of inkjet inks in the textile industry is forecasted to reach 17.5 % from 2024 to 2029, clearly showing its brilliant perspective [1-9].

Inkjet inks are divided into two types based on the colorants used: dye-based and pigment-based inks. Although dye-based inks continue to dominate some applications, pigment-based inks have progressively expanded their market share since the late 1980s, particularly in response to the growing need for better light and wash fastness in inkjet-printed items [7]. However, formulating pigment-based inkjet inks is more demanding, as it requires highly stabilized, low particle size dispersion of pigment particles in the ink medium. Maintaining particle size during application and storage is crucial to prevent clogging of the tiny nozzles and channels [7, 10]. Given the small size of these nozzles and channels, it is widely recognized that the particle size of pigment-based inkjet inks should be less than 450 nm, and preferably below 200 nm, after production, during storage, and application. This requirement can be fulfilled by surface modification of the pigments, either chemically [11] or physically [12-14].

Polymeric dispersants play a vital role in dispersing and stabilizing pigment particles in the ink medium via physical modification approach [15-19]. These macromolecules contain pigment-affinic groups, or anchors, that attach to the particle surfaces, while soluble segments in the media create electrostatic repulsion or steric hindrance, preventing particle agglomeration [20-27]. Although polymeric dispersants provide essential stabilization for dispersed particles, their high molecular weight results in slower absorption onto the particle surfaces. Conversely, surfactants, being smaller molecules, are kinetically more favorable for absorption onto the pigment surface. They are added to improve the wettability of the particles and reduce the milling time required to achieve appropriate particle sizes, while also helping to adjust the surface tension of the ink [23, 28-30]. While the presence of surfactants and polymeric dispersants is crucial for achieving an optimal dispersion state, their interdependence complicates the dispersion and stabilization of pigment-based inkjet inks, as they affect one another's performance.

In addition to the particle size of pigments and their stability in the ink, the overall performance of inkjet printing inks heavily relies on the interplay between rheological behavior and surface tension, both significantly affected by polymeric dispersants and surfactants. Accordingly, it is believed that the printability of ink can be roughly predicted by considering its Weber number (We), which relates to surface tension, and its Reynolds number (Re), which describes flow behavior. Therefore, the development of pigment-based inkjet inks must ensure that rheological behaviors and surface tension meet the stringent requirements for inkjet inks [31-34]. This complexity arises from the inevitability of incorporating surfactants and polymeric dispersants, which not only directly affect flowability and surface behavior but also influence these characteristics by modifying the state of dispersion. Particle size distribution and interparticle interactions significantly influence the rheological properties and surface tension characteristics of the ink. Both the molecular structure and quantities of dispersants and surfactants in the formulation influence the overall performance of the ink [35-37].

The effects of polymeric dispersant and surfactant combinations on the properties of aqueous pigment-based inkjet inks have been thoroughly scrutinized to address these issues. Different surfactants and various polymeric dispersant concentrations have been studied to achieve proper dispersion of Disperse Blue 359, a well-known pigment for sublimation transfer inkjet inks, while maintaining the formulation's flowability and surface tension within appropriate ranges for inkjet applications.

2. Experimental

2.1. Materials and instruments

DISPERBYK® 2015 (PolyD2015), a 40 *wt.*% aqueous solution of modified styrene-maleic anhydride copolymer was purchased from BYK company. Oleic acid ethoxylate (6 moles, KEOL6), oleic acid

ethoxylate (9 moles, KEOL9), and nonyl phenol ethoxylate (10 moles, KENON10) were all provided by Kimyagaran Emrooz company. Disperse Blue 359 (D.B.359) was supplied by Tiankum Company. Ethylene glycol (99.5 %), glycerol (99.5 %), and propylene glycol (99 %) were obtained from Merck Company.

Surface tension measurements were conducted with a Kruss tensiometer using the Wilhelmy plate method. Particle size distribution was measured using the Horiba SZ-100 instrument. Rheological properties were evaluated using the MCR300 Physica Anton par with concentric cylinder, which enabled assessment of ink flow behavior and viscosity. The accuracy of viscosity measurement was assessed, and the error margin for rheological measurements was found to be less than 0.5 mPas. Turbidity measurements during milling and storage were conducted with a Hach 2100N instrument, providing data on milling effectiveness and ink stability during storage. The accuracy of turbidity measurement was also assessed, and the error margin was found to be less than 3 NTU.

2.2. Sample preparation

This study was conducted in two phases. In the first phase, the impact of various surfactants on the milling process and milling paste characteristics were investigated. Mill base formulations with different surfactants were prepared, as detailed in Table 1. The mill base preparation involved dissolving the appropriate amounts of polyD2015, surfactant, and propylene glycol in deionized water using a magnetic stirrer. Once complete dissolution was achieved, D.B.359 was gradually added to the stirring solution, and stirring continued for an additional 60 minutes to ensure thorough wetting of the dye particles. Subsequently, 25 g of the mill base was poured into the milling vessel along with 190 g of zirconia grinding media (0.8-1 mm diameter). Milling was conducted using a jar mill at 175 rpm for 120 hours.

Upon determining the surfactant with the best performance, the second phase of the study aimed to optimize the concentration of the polymeric dispersant. Accordingly, samples with the most efficient surfactant and varying amounts of polyD2015 were prepared based on the formulations in Table 2. The nomenclature of samples is based on the weight ratio of the solid polymeric dispersant to the pigment. The mill base preparation followed the procedure used in the first phase of the study.

Table 1: Sample formulations for determining the proper surfactant.

Sample name	polyD2015 (g)	KEOL6 (g)	KENON10 (g)	KEOL9 (g)	Glycerol (g)	PG (g)	D.B.359 (g)	Water (g)
Blank	2.5	–	–	–	1	1	2	6.25
Kl6	2.5	0.1	–	–	1	1	2	6.15
Kn10	2.5	–	0.1	–	1	1	2	6.15
Kl9	2.5	–	–	0.1	1	1	2	6.15

Table 2: Sample formulations for optimizing the dispersing agent content.

Sample name	D.B.359 (g)	polyD2015 (g)	surfactant (g)	Glycerol (g)	PG (g)	Water (g)
S-25	2	1.25	0.1	1	1	8.75
S-50	2	2.5	0.1	1	1	7.5
S-75	2	3.75	0.1	1	1	6.25
S-100	2	5	0.1	1	1	5
S-125	2	6.25	0.1	1	1	3.75
S-150	2	7.5	0.1	1	1	2.5

3. Results and Discussions

3.1. The effect of surfactant nature

Various behaviors of inkjet inks during production, droplet formation, droplet transfer, and interactions with substrates are significantly influenced by surfactants. During the production of the mill base, surfactants lower surface tension, allowing the mill base media to penetrate the grooves and crevices of pigment aggregates and agglomerates. This enhancement in wetting improves the efficiency of the milling process and reduces its duration. Furthermore, better wetting minimizes interactions between suspended particles, which is reflected in the rheological properties. Interparticle interactions lead to energy dissipation during flow, causing the fluid to exhibit non-Newtonian behavior. Consequently, the effects of various surfactants on the surface tension and rheological behavior of mill bases have been studied to identify the most effective option [5, 38]. Measurements were taken to examine how the surfactant structure and the milling process affect the surface tension of the mill base (Table 3).

As shown, the addition of pigment to the media does not significantly affect the surface tension of the samples unless milling occurs. Grinding the large pigment particles during the milling process increases their surface area, allowing for greater surfactant absorption. This results in a lower amount of unabsorbed surfactant in the media and thus an increase in surface tension. However, before milling, significant surfactant absorption does not occur on the pigment surface due to its low surface area, leaving the surface tension unchanged. Moreover, the surface tension of the samples is also influenced by the intrinsic characteristics of the surfactants, as detailed in Table 4.

Surfactants can greatly affect the kinetics of dispersion since they are kinetically more favorable than polymeric dispersants to absorb on the particle surface owing to their low molecular weight. Therefore, they greatly enhance surface wetting, the first step of dispersion. To find out which surfactant enhances milling kinetics more efficiently, the evolution of sample turbidity during the milling process has been monitored using turbidimetry. Comparing the turbidity of samples with the same pigment and concentration provides insight into their particle size [36, 39-41]. Turbidity was recorded after 24 hours of milling, as indicative of the initial rate of particle size reduction and after 120 hours as the ultimate particle size reduction efficiency. As depicted in Table 4, Kl6 greatly enhances the milling rate compared with other samples. Given that Blank exhibits the highest turbidity at the initial stage of milling, it can be also deduced that all the surfactants improve the dispersion kinetics by enhancing the wetting process.

Table 3: Effect of surfactant structure and milling process on the surface tension of the mill base.

Sample	pigment-free media (mN/m)	mill base before milling (mN/m)	mill base after milling (mN/m)
Blank	43.437 ± 0.5	43.491 ± 0.5	47.919 ± 0.5
Kl6	35.147 ± 0.5	35.217 ± 0.5	39.381 ± 0.5
Kl9	38.512 ± 0.5	38.630 ± 0.5	42.041 ± 0.5
Kn10	33.965 ± 0.5	33.841 ± 0.5	38.137 ± 0.5

Table 4: Turbidity evolution of samples with different surfactants during milling.

Sample	Blank	Kn10	Kl6	Kl9
Turbidity after 24 (NTU)	5384 ± 3	4671 ± 3	3232 ± 3	4246 ± 3
Turbidity after 120 (NTU)	1352 ± 3	1023 ± 3	565 ± 3	793 ± 3

The stability of pigment dispersion is also of great importance. The particle size of samples during storage time after milling was also assessed using turbidimetry. The turbidimetric evaluation was conducted to investigate the stability of the samples after milling. In this regard, the samples were stored after milling, and their turbidity was measured over a prolonged time. The changes in turbidity over time are represented in Figure 1. It can be seen that Kl6 has the smallest and most stable pigment particles, exhibiting the lowest turbidity, which remains constant throughout the storage period. Kl9 shows a nearly stable dispersion; yet, its higher turbidity than Kl6 suggests a larger particle size. Blank and Kn10 not only exhibit larger particle sizes, as indicated by their high turbidity but also exhibit stability issues, as reflected in their fluctuating turbidity over time. The decreasing turbidity of Blank and Kn10 during storage can be attributed to the sedimentation of pigment particles, which consequently reduces the concentration of scattering particles in the samples.

The particle size of samples was also assessed using turbidimetry. Comparing the turbidity of samples with the same pigment and same concentration can give an insight into their particle size. The turbidimetric evaluation was also conducted to investigate the stability of the samples after milling. In this regard, samples were stored after milling, and their turbidity was measured over a prolonged storage time. The turbidity changes of samples over time are represented in Figure 1. It can be seen that Kl6 has the smallest and most stable pigment particles. It has the lowest turbidity which remains constant over storage time. Kl9 has almost stable dispersion however, its higher turbidity in comparison with Kl6, denotes its larger particle size. Blank and Kn10 not only have large particle sizes, which is indicated by their high turbidity but also, have stability issues which are depicted in their deviating turbidity over time. The reducing turbidity of Blank and Kn10 over storage time can be attributed to the sedimentation of pigment particles, which consequently reduces the concentration of scattering particles in the samples.

The state of dispersion is reflected in the rheological behavior. The layer of dispersing and wetting agents absorbed on the pigment particles prevents flocculation by reducing interparticle interactions, thereby stabilizing them in the media [42-44]. Limiting these interactions also affects the fluid's response to applied shear forces. Dispersions with high interparticle interactions exhibit viscoelastic behavior, while those with minimal interactions display nearly Newtonian rheological properties. Furthermore, reducing interparticle interactions in pigment dispersions leads to lower viscosity, which is critical for inkjet inks to ensure proper droplet formation and transfer to the substrate [45, 46]. Consequently, the rheological characteristics of the samples have been investigated.

A four-step testing approach was used to assess the rheological behavior of the inkjet ink samples. To eliminate residual rheological effects in the samples from prior processes, every sample was first subjected to a pre-shear treatment. The pre-shear treatment includes one minute of exposure to a shear rate of 100 s^{-1} which is followed by two minutes of rest. This way, the viscosity of the samples at low shear rates as well as its stability over time have been assessed. After these two steps, a shear sweep test has been conducted in both loading and unloading mode.

During the loading phase, measurements of the shear sweep were performed by gradually increasing the shear rates from 0.01 to 1000 s^{-1} over one minute. This process enabled the evaluation of how the viscosity of the ink responded to escalating shear conditions. After the loading phase, the unloading phase commenced, where shear rates were reduced from 1000 s^{-1} back to 0.01 s^{-1}, also over one minute. This phase offered valuable insights into the viscoelastic characteristics of the ink and its capacity to revert to its original rheological state after being subjected to high shear rates. [19, 29].

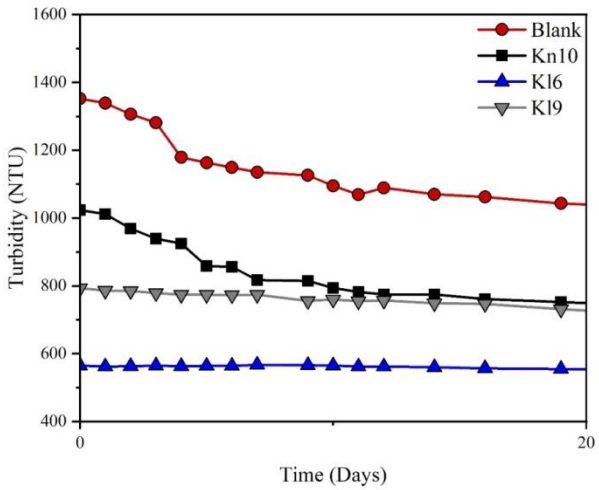

Figure 1: Turbidity evolution of samples with different surfactants, during storage.

The viscosity of Newtonian fluids is independent of time or shear rate. Consequently, at the initial stage of rheological assessment, the viscosity at 100 s^{-1} over time was measured. As illustrated in Figure 2, Kl6 and Kl9 maintain stable viscosity at 100 s^{-1}, while Kn10 and the blank sample exhibit significant viscosity variations over time. Additionally, Kl6 displays the lowest viscosity. The average viscosity at 100 s^{-1} is summarized in Table 5.

The rheological behavior of samples with various surfactants in loading and unloading modes are shown in Figure 3. As can be observed, Kl6 exhibits nearly constant viscosity over various shear rates, while Blank, Kl9, and Kn10 show shear thinning behavior (Table 6).

Rheological hysteresis represents the extent of energy dissipation upon the flow of the fluids. It describes the discrepancy in the behavior of viscoelastic fluids during the loading and unloading phases of cyclic strain sweeps, which stems from energy dissipation caused by particle interactions. A lower rheological hysteresis signifies reduced particle interactions and improved dispersion [47, 48]. As shown in Table 6, Kl6 exhibits very low hysteresis, verifying its superior dispersion quality. Given that the hydrophilic-lipophilic balance (HLB) of KEOL6, KENON10, and KEOL9 are 9.9, 13.4, and 11.6, respectively.

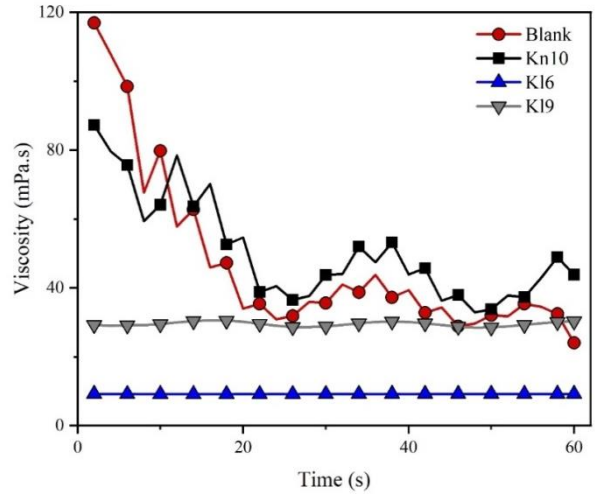

Figure 2: Viscosity of samples with different surfactants at 100s^{-1}, over time.

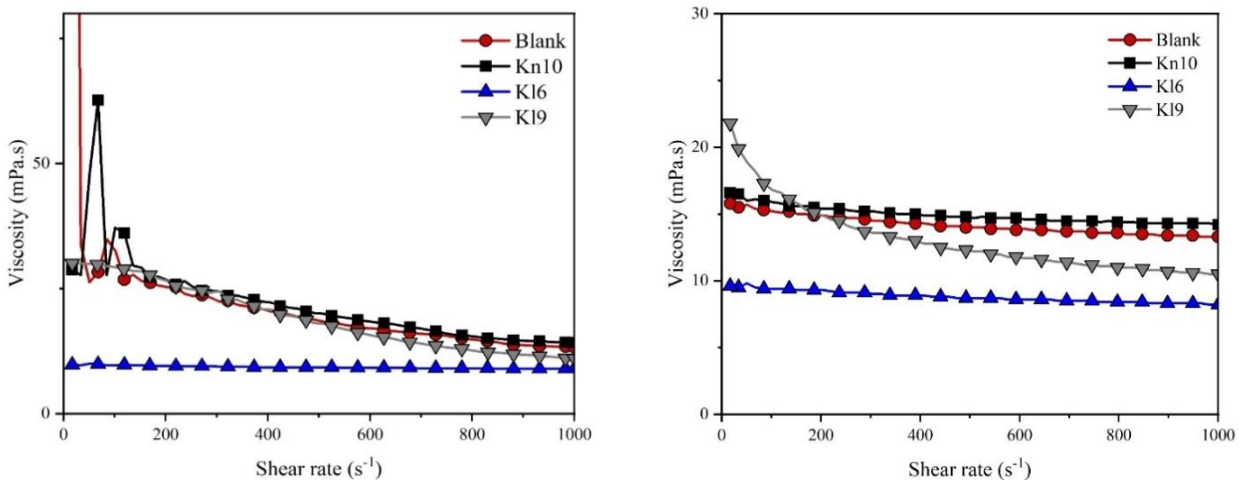

Figure 3: Viscosity of the samples with different surfactants as a function of shear rate in (up) loading mode and (down) unloading mode.

Table 5: Effect of surfactant on the viscosity at 100 s^{-1}.

Sample	Blank	Kn10	Kl6	Kl9
Viscosity (mPa.s)	46.78	50.69	9.17	28.59

Table 6: Rheological hysteresis of samples with various surfactants.

Sample	Blank	Kn10	Kl6	Kl9
Rheological hysteresis	8221.11	6926.48	665.98	6062

It seems that the tendency of KEOL6 to remove from the solution and absorb on the particle surface is higher in comparison to the two other surfactants, which can explain the lower hysteresis, lower viscosity, and more Newtonian behavior in Kl6 rather than Kl9 and Kn10. It can also explain the superior performance of KEOL6 over other surfactants in enhancing milling rate (Table 4) since it has more tendency to absorb on the particle surface and improve its wetting.

3.2. The effect of dispersant concentration

In addition to the surfactant structure, the concentration of dispersant significantly influences the performance of pigment-based inkjet inks. It is well established that excessive amounts of polymeric moieties in inkjet formulations can cause the system to transition from a dilute regime to semi-dilute and concentrated regimes, leading to significant interactions between polymer chains. This is an undesirable situation for inkjet applications, as it can deviate their rheological performance from that of Newtonian fluids [49]. Moreover, incorporating an excessive quantity of polymeric dispersant adversely affects the state of dispersion by suppressing both electrostatic and steric hindrance mechanisms that stabilize particles. A surplus of charge-bearing polymeric dispersants can form a thick layer on the particle surface, neutralizing its surface charge [50]. This can also lead to an increase in unabsorbed polymer chains in the solution, which may induce depletion flocculation and further suppress steric hindrance [51-53]. Conversely, insufficient amounts of polymeric dispersant can leave parts of the particle surface uncovered, resulting in flocculation [53]. Therefore, optimizing the dispersant concentration is crucial. To identify the optimal dispersant concentration, samples with varying amounts of dispersant were prepared. In all samples, Kl6, which has demonstrated superiority over the other two counterparts, was used as the surfactant.

The influence of polymeric dispersant concentration on the dispersion of pigment in the media has been thoroughly analyzed. Particle size was first assessed using DLS. As shown in Figure 4, increasing the concentration of PolyD2015 up to 50 % of the pigment reduces the particle size, while further increments lead to an increase in particle size. Incorporating PolyD2015 up to 75 % of pigment weight still keeps the particle size below 250 nm which is acceptable for inkjet inks; however, samples containing 100 % or more of PolyD2015 exhibit bimodal particle size distribution, with the first peak below 500 nm and a second peak larger than one micron. Finally, S-150 only shows a peak in the micron range.

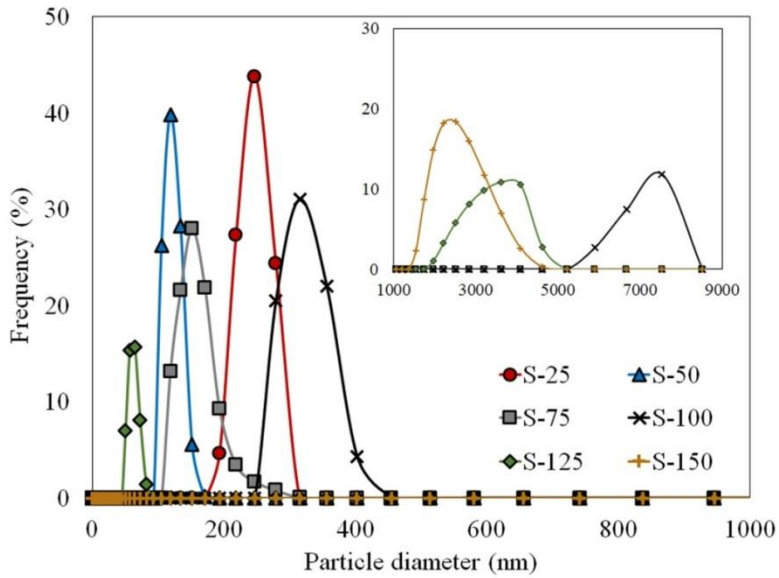

Figure 4: The effect of polymeric dispersant concentration on the particle size distribution and (inset) particle size in the micron range.

To understand the effect of polymeric dispersant on the dispersion stability of the pigment, the turbidity of the samples over prolonged storage time has been monitored. The turbidity deviation of samples over time is represented in Figure 5. As seen, the S-50 has the lowest and most stable turbidity over time. S-75 also shows low turbidity variation, indicative of its stability, however, its turbidity is higher than S-50 which demonstrates its higher particle size. S-20 displays a markedly different turbidity profile over time, with an initial turbidity significantly higher than that of S-50 and S-75. Moreover, it exhibits a rapid increase in the first days of storage which is followed by a swift decrease. As the milling proceeds, pigment aggregates, and agglomerates continue to break down, which provides a new, fresh surface for dispersants and surfactants to absorb. If the dispersant concentration is insufficient, some parts of the surface remain uncovered and susceptible to flocculation. Applied shear forces during milling can mitigate flocculation tendencies, but in the absence of such forces during storage, particles rapidly flocculate, leading to increased turbidity. The flocculated particles eventually precipitate, resulting in a significant decrease in overall turbidity. In S-100, S-125, and S-150, different behaviors are observable. In these samples, turbidity first starts to reduce consistently at a considerable rate that can be attributed to the precipitation of large particles-their presence has already been indicated by DLS. This initial steady decrease is followed by a rapid increase and then a decrease in turbidity. It can be interpreted as the formation and then precipitation of particle flocculation since, excessive polymeric dispersant deteriorates dispersion stability by neutralizing particles surface charge -which is the main stabilization mechanism of PolyD2015- and depletion-induced phenomenon.

Dispersion efficiency is also well represented in rheological behavior. The standard four-step rheological measurement is carried out on the samples with various dispersant concentrations as described earlier in this article. The viscosity of the samples at the shear rate of 100 s^{-1} over time is represented in Figure 6. S-50 exhibits the lowest viscosity and also the highest viscosity consistency over time. Increasing the amount of dispersant causes the viscosity to increase gradually from S-75 to S-150. It can be attributed to the rise up of unabsorbed polymer chains in the solution. The rheological evaluation of the samples in shear sweeping mode, in both the loading and unloading phase (Figure 7) further reveals that S-50 shows the highest resemblance to Newtonian fluids. The rheological hysteresis of this sample is also lower than others as shown in Table 7, confirming the superior dispersion quality of S-50 compared to the other samples. It is also noticeable that passing dispersant to pigment ratio above of 75 %, further incorporation of dispersant causes the rheological hysteresis to decrease. It is in good alliance with DLS findings which confirmed the presence of large micron-size pigment clusters in these samples. Larger particle sizes in these samples provide smaller surface area and hence lower interaction between particles surfaces. It can explain their lower rheological hysteresis in comparison with S-25 and S-75, in which a tiny coincidence of small particle size and appropriate dispersing agent concentration, causes significant interactions.

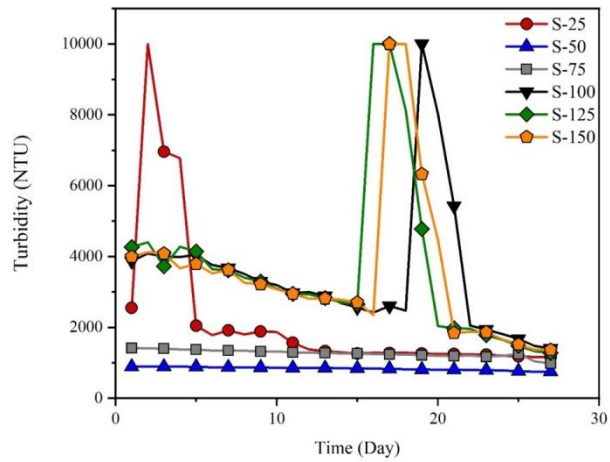

Figure 5: Turbidity of the samples with various amounts of polymeric dispersant, over time.

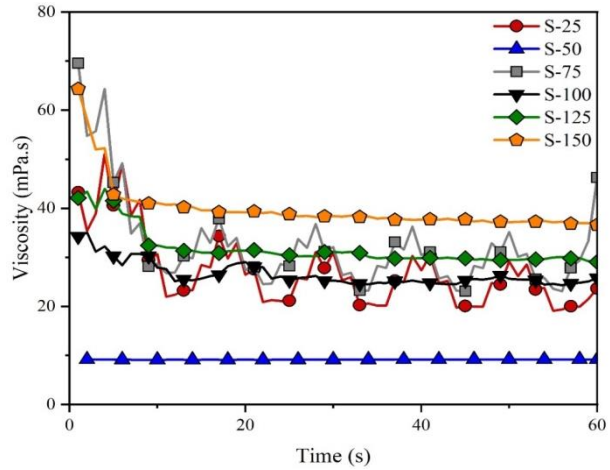

Figure 6: Viscosity of samples with various amounts of polymeric dispersants at 100 s^{-1}.

Table 7: Rheological hysteresis of samples with various amounts of polymeric dispersants.

Sample	S-25	S-50	S-75	S-100	S-125	S-150
Rheological hysteresis	4953.77	665.98	3708.2	2299.68	1342.09	1521.58

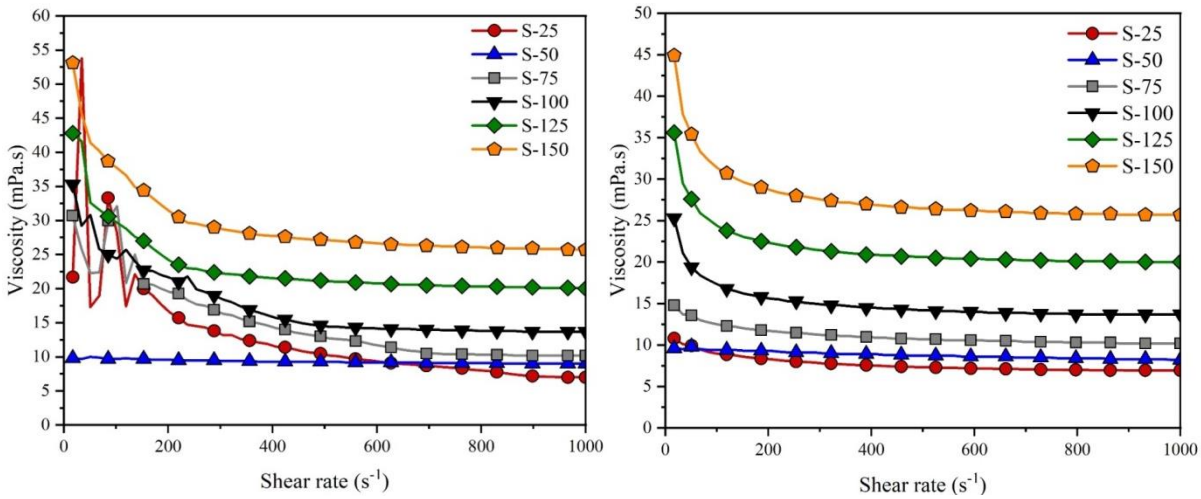

Figure 7: Viscosity of the samples with various amounts of polymeric dispersant as a function of shear rate in (up) loading mode and (down) unloading mode.

Table 8: viscosity of samples with various amounts of polymeric dispersants at 1000 s^{-1}.

Sample	S-25	S-50	S-75	S-100	S-125	S-150
viscosity (mPa.s)	6.95	8.21	10.2	13.7	20	25.7

The viscosity of samples at 1000s^{-1} is also represented in Table 8. It is evident that increasing the amount of polymeric dispersant in the formulation, causes the viscosity to grow up. This trend has not seen at 100s^{-1} (Figure 7). It seems that at high shear rates, most of the interparticle interactions have been disappeared and only the interactions attributed to the polymeric chains are remained, while at low shear rates, interparticle interactions are predominant. The higher viscosity of the samples at high shear rates can explain the presence of micron-size particles in the samples with excessive amount of polymeric dispersant which was revealed by DLS. Milling was carried out using jar mill, a low energy milling method. The milling efficiency of a jar mill is heavily dependent on factors such as jar size, rotation speed, media size, density, volume fraction of milling media, and the viscosity of the mill base. High-viscosity mill bases impede the transfer of energy from the milling media to the particles, thus reducing their mobility. S-100, S-125, and S-150 exhibit high viscosity and cannot be effectively ground in the jar mill, resulting in the presence of some larger, unground pigment particles. These non-ground particles contribute to the second peak in their bimodal particle size distribution curves.

4. Conclusion

In developing aqueous pigment-based inkjet inks various issues have to be addressed, among which, dispersion and printability are paramount. Pigment-based inkjet inks should have particle sizes of less than 250 nm and maintain stability during storage and application. Furthermore, obtaining optimum printability necessitates a delicate balance between rheological characteristics and surface tension. This issue is challenging to overcome since dispersing agents and surfactants predominantly affect dispersion and simultaneously interact and influence both rheological behavior and

surface tension directly and through their effects on the state of dispersion.

In pursuit of a scientific method for optimizing polymeric dispersant/surfactant combinations in the formulation of aqueous pigment-based inkjet inks, various formulations have been developed. Among different surfactants, it was found that Kl6 provided the best rheological behavior, which means low viscosity with the lowest dependency on either the size or duration of shear. It also exhibited the best performance on improving milling kinetics and dispersion stability which was verified by turbidimetry. The superior performance of Kl6 was attributed to its lower HLB and higher tendency to absorb on the pigment surface.

The study then continued by exploring the optimal polymeric dispersant concentration in the presence of Kl6. DLS showed that the tiniest particles with the most uniform distribution were obtained at a surfactant to pigment ratio of 50 %. Sample with dispersant to pigment ratio below 50 % had larger particle sizes while ratios above 75 %, had bimodal particle size distribution curves with a peak in the micron range. Monitoring the turbidity over time indicated that S-50 also exhibits the best dispersion stability over time.

Rheological assessment confirms the superiority of S-50 in terms of the state of dispersion. The sample had the lowest viscosity while its viscosity was almost independent of the duration and size of the applied shear which is the confirmation of its Newtonian rheological behavior. Furthermore, S-50 had the lowest rheological hysteresis, all indicating minimal interparticle interaction. S-25 on the other hand shows very low dispersion stability but maintained sub-micron particle size. It also shows the highest rheological hysteresis suggesting insufficiency of dispersant in this sample for covering the new surfaces generated during milling, leading to flocculation of the ground pigment particles.

Given their high viscosity and the presence of large pigment clusters, samples with a dispersant to pigment concentration above 75 % are considered too viscous to be properly milled by low-shear methods such as jar milling. The excessive amount of polymeric dispersant in these samples likely shifts them from a dilute to a semi-concentrated regime, which prevents the milling beads from effectively impacting and breaking the clusters, leaving some agglomerates unground. Additionally, the excessive polymer dispersant not only impairs the milling process by increasing polymer chain entanglement but also deteriorates the stability of the dispersion through various mechanisms, as evidenced by zeta potential and turbidimetry measurements. These findings shed light on how to formulate high-performance pigment-based inkjet inks, emphasizing the interplay between dispersants and surfactants in obtaining maximum printability and stability.

5. References

1. Kosolia CT, Tsatsaroni EG, Nikolaidis NF. Disperse ink-jet inks: properties and application to polyester fibre. Color Technol. 2011; 127(6):357-64. https://doi.org/10.1111/j.1478-4408.2011.00334.x.
2. Kosolia CT, Varka EM, Tsatsaroni EG. Effect of surfactants as dispersing agents on the properties of microemulsified inkjet inks for polyester fibers. J Surfact Detergent. 2011; 14(1):3-7. https://doi.org/10.1007/s11743-010-1194-7.
3. Gao C, Wang H, Zhao H, Shi S, Guo H, Wang S, Fan L. Study on the quality and inkjet printing effect of the prepared washing-free disperse dye ink. RSC Adv. 2023; 13(18):12141-52. https://doi.org/10.1039/D3RA01597A.
4. Mousazadeh M, Khademi N, Kabdaşlı I, Rezaei S, Hajalifard Z, Moosakhani Z, Hashim K. Domestic greywater treatment using electrocoagulation-electro-oxidation process: optimisation and experimental approaches. Sci Rep. 2023; 13(1):15852. https://doi.org/10.1038/s41598-023-42831-6.
5. Li L, Chu R, Yang Q, Li M, Xing T, Chen G. Performance of washing-free printing of disperse dye inks: influence of water-borne polymers. Polymers. 2022; 14(20):4277. https://doi.org/10.3390/polym14204277.
6. Research S. Digital Textile Printing Inks Market Size, Share, Trends, Forecast, & Growth Analysis-2024-2029. Michigan, United states: Stratview Research:2023. https://www.stratviewresearch.com/324/Digital-Textile-Printing-Inks-Market.html.
7. Kamyshny A, Sowade E, Magdassi S. Inkjet ink formulations: overview and fundamentals. In: Zapka W. (eds.) Inkjet Printing in Industry. Weinhein, Germany: Wiley-VCH GmbH; 2022.
8. Hutchings IM, Martin GD, Hoath SD. Introductory Remarks, In: Hoath SD. (eds.) Fundamentals of Inkjet Printing. Winheim, Germany: Wiley-VCH Verlag GmbH & Co. KGaA; 2016.
9. Hajalifard Z, Mousazadeh M, Khademi S, Khademi N, Jamadi MH, Sillanpää M. The efficacious of AOP-based processes in concert with electrocoagulation in

abatement of CECs from water/wastewater. Clean Water. 2023; 6(1):30. https://doi.org/10.1038/s41545-023-00239-9.
10. Kipphan H. Fundamentals, In: Kipphan H. Handbook of Print Media: Technologies and Production Methods. Berlin, Heidelberg: Springer Berlin Heidelberg; 2001.
11. Nie L, Xu X, Chen Y, Dong Y, Chang G, Li R. Development of binder-free pigment inks for direct inkjet printing on cotton fabric without pretreatment. Langmuir. 2023; 39(17):6266-75. https://doi.org/10. 1021/ acs.langmuir.3c00573.
12. Nayini MMR, Ranjbar Z. Carbon nanotubes: dispersion challenge and how to overcome it, In: Abraham J, Thomas S, Kalarikkal N. (eds.) Handbook of carbon nanotubes. Cham: Springer Int Publishing; 2022.
13. Yuan J, Xu J. Synthesis of amphiphilic block copolymer and its application in pigment-based ink. Materials. 2024; 17(2):330. https://doi.org/ 10.3390/ma 17020330.
14. Asada M, Tanaka H, Suwa Y, Osawa S, Otsuka H. Improved pigment dispersibility in thick inks based on increased molecular dispersion of poorly water-soluble block copolymers. Dyes Pigm. 2024; 226112140. https://doi.org/10.1016/j.dyepig.2024.112140.
15. Augé J, Leroy F. Lithium trifluoromethanesulfonate-catalysed aminolysis of oxiranes. Tetrahedron Lett. 1996; 37(43):7715-6. https://doi.org/10.1016/0040-4039 (96)01731-5.
16. Yoon C, Choi JH. Synthesising polymeric dispersants to apply to carbon black pigmented mill bases for use in ink-jet inks. Color Technol. 2020; 136(1):60-74. https:// doi.org/10.1111/cote.12446.
17. [17]Biswas A, Sharma BK, Willett JL, Erhan SZ, Cheng HN. Soybean oil as a renewable feedstock for nitrogen-containing derivatives. Energy Environ Sci. 2008; 1(6):639-44. https://doi.org/10. 1039/ B809215J.
18. Mohammad Raei Nayini M, Jalili M, Ranjbar Z. Printed electronics based on carbon nanotubes and graphene nanosheets. J Studies Color World. 2020; 10 (3): 29-42.https://dorl.net/dor/20.1001.1.22517278.1399. 10.3.3.8.
19. Mohammad raei Nayini M, Jalili M, Bastani S, Khamseh S. Printed solar cells an inevitable remedy for the global energy crisis. J Studies Color World. 2023; 13(4):377-406. https://dorl.net/dor/20.1001.1.22517278. 1402.13.4.3.1.
20. Auschra C, Eckstein E, Mühlebach A, Zink MO, Rime F. Design of new pigment dispersants by controlled radical polymerization. Prog Org Coat. 2002; 45(2):83-93. https://doi.org/10.1016/S0300-9440(02) 00048-6.
21. Van den Haak HJW. Design of pigment dispersants: methodology for selection of anchoring groups. J Coat Technol. 1997; 69(873):137-42. https://doi.org/10.1007/ BF02697764.
22. Najafi F, Shirkavand Hadavand B, Manouchehri F. Synthesis and characterization of anionic polyurethane dispersants for waterborne paints. Prog Color Colorant Coat. 2013; 7(3):147-54. https://doi.org/10.30509/ pccc. 2013. 75835.
23. Meghdadi Esfahani F, Balali E, Hashemi SS, Khadivi R, Mohammad Raei Nayini M, Voung B. Investigating an iron-doped fullerene cage for adsorption of niacin (vitamin B3): DFT analyses of bimolecular complex formations. Comput Theor Chem. 2022; 1214113768. https://doi.org/10.1016/j.comptc.2022.113768.
24. Hayeri T, Mannari V. Sustainable organic–inorganic hybrid coating system with multiple cure capabilities. J Coat Technol Res. 2024; https://doi.org/10.1007/ s11998-024-00969-6.
25. Mohammad Raei Nayini M, Bastani S, Moradian S, Croutxé-Barghorn C, Allonas X. Manipulating the surface structure of hybrid UV curable coatings through photopolymerization-onduced phase separation: influence of inorganic portion and photoinitiator content. Macromol Chem Phys. 2018; 219(4):1700377. https:// doi.org/10.1002/macp.201700377.
26. Raoufi F, Montazeri S, Rastegar S, Asadi S, Ranjbar Z. Dispersion of silica aerogel particles in thermal insulating waterborne coating. Prog Color Colorant Coat. 2023; 16(3):309-17. https://doi.org/10.30509/ pccc.2023.167112.1206.
27. Motamedi M, Ashhari S, Nayini MMR, Ranjbar Z, Optical electrical and mechanical properties of functionalized polymer nanocomposites. In: Patel G, Deshmukh K, Hussain CM. (eds.) Advances in Functionalized Polymer Nanocomposites. Cambridge-United States: Woodhead Publishing; 2024.
28. Abreu B, Pires AS. Guimarães A, Fernandes RMF, Oliveira IS, Marques EF. Polymer/surfactant mixtures as dispersants and non-covalent functionalization agents of multiwalled carbon nanotubes: Synergism, morphological characterization and molecular picture. J Mol Liq. 2022; 347118338. https://doi.org/10.1016/j. molliq.2021.118338.
29. Chang CJ, Chang SJ, Tsou S, Chen SI, Wu FM, Hsu MW. Effects of polymeric dispersants and surfactants on the dispersing stability and high-speed-jetting properties of aqueous-pigment-based ink-jet inks. J Polym Sci Part B: Polym Phys. 2003; 41(16):1909-20. https://doi. org/ 10.1002/polb.10562.
30. Mohsen MRN, Mojtaba J, Zahra R. Printed electronics, based on carbon nanotubes and graphene nanosheets. J Studies Color World. 2020; 10(3):29-42. https://dor.net/20.1001.1.22517278.1399.10.3.3.8.
31. Fromm JE. Numerical calculation of the fluid dynamics of drop-on-demand jets,. IBM J Res Dev. 1984; 28(3):322-33. 10.1147/rd.283.0322.
32. Derby B, Reis N. Inkjet printing of highly loaded particulate suspensions. MRS Bull. 2003; 28(11):815-8. https://doi.org/10.1557/mrs2003.230.
33. Reis N, Ainsley C, Derby B. Ink-jet delivery of particle suspensions by piezoelectric droplet ejectors, J Appl Phys. 2005; 97(9):094903. https://doi.org/10. 1063/1.1888026.
34. Gaida R, Dziubek K, Król K, Ostaszewska M, Wit M. Influence of different dispersants on the quality and

stability of aqueous quinacridone magenta pigment dispersion for ink-jet applications. Color Technol. 2023; 139(6):637-53. https://doi.org/10.1111/cote.12678.
35. Alihoseini MR, Khani MR, Jalili M, Shokri B. Direct sublimation inkjet printing as a new environmentally friendly approach for printing on polyester textiles. Prog Color Colorant Coat. 2021; 14(2):129-38. https://doi. org/10. 30509/pccc.2021.81699.
36. Gharanjig H, Gharanjig K, Sarli MA, Ozguney AT, Jalili M, Gharanjik A, Jahankaran S. Effect of molecular composition of comb-like polycarboxylate dispersants on hydrophobic dye dispersion properties, J Mol Liq. 2022;350118615. https://doi.org/10.1016/j.molliq. 2022. 118615.
37. Mohammad Raei Nayini M, Bastani S, Ranjbar Z. Synthesis and characterization of functionalized carbon nanotubes with different wetting behaviors and their influence on the wetting properties of carbon nanotubes/polymethylmethacrylate coatings. Prog Org Coat. 2014; 77(6):1007-14. https://doi.org/10.1016/ j. porgcoat.2014.02.013.
38. Abdelaziz MA, Ibrahim MA, Abdel-Messih MF, Mekewi MA. Vivid application of polyurethane as dispersants for solvent based inkjet ink. Prog Org Coat. 2020;148105875.https://doi.org/10.1016/j.porgcoat.2020 . 105875.
39. Chung YS. Turbidimetric evaluation of the dispersion properties of disperse dyes. Text Res J. 2000; 70(6):550-4. 10.1177/004051750007000613.
40. Rust S, Pauer W. Determination of inline-particle sizes by turbidity measurement in high solid content emulsion polymerisations. J Polym Res. 2022; 29(7):307. https://doi.org/10.1007/s10965-022-03141-z.
41. Seneewong-Na-Ayutthaya M, Pongprayoon T, O'Rear EA. Colloidal stability in water of modified carbon nanotube: comparison of different modification techniques. Macromol Chem Phys. 2016; 217(23):2635-46. https://doi.org/10.1002/macp.201600334.
42. Shen X, Sun X, Liu J, Hang J, Jin L, Shi L. A facile strategy to achieve monodispersity and stability of pigment TiO_2 particles in low viscosity systems. J Colloid Interface Sci. 2021; 581586-94. https://doi.org/ 10.1016/j.jcis.2020.07.132.
43. Dybowska-Sarapuk L, Kielbasinski K, Arazna A, Futera K, Skalski A, Janczak D, Sloma M, Jakubowska M. Efficient inkjet printing of graphene-based elements: influence of dispersing agent on ink viscosity. Nanomaterials. 2018; 8(8):602. https://doi.org/10. 3390/ nano8080602.
44. Gebauer JS, Mackert V, Ognjanović S, Winterer M. Tailoring metal oxide nanoparticle dispersions for inkjet printing. J Colloid Interface Sci. 2018; 526400-9. https://doi.org/10.1016/j.jcis.2018.05.006.
45. Nallan HC, Sadie JA, Kitsomboonloha R, Volkman SK, Subramanian V. Systematic design of jettable nanoparticle-based inkjet inks: rheology acoustics and jettability. Langmuir. 2014; 30(44):13470-7. https://dpi. org/ 10.1021/la502903y.
46. Tuladhar T. Measurement of complex rheology and jettability of inkjet inks. In: Handbook of Industrial Inkjet Printing. 2017.
47. Mohammad Raei Nayini M, Ataeefard M. Characterization of electrophotographic printing toner: thermomechanical point of view. Prog Color Colorant Coat. 2024;17(2):175-83. https://doi.org/10.30509/ pccc. 2023.167163.1232.
48. Ziegelbaur RS, Caruthers JM. Rheological properties of poly(dimethylsiloxane) filled with fumed silica: I. Hysteresis behaviour. J Non-Newtonian Fluid Mech. 1985; 17(1):45-68. https://doi.org/10.1016/0377-0257 (85) 80005-7.
49. Wheeler JSR, Yeates SG, Polymers in inkjet printing. In: Hoath SD. Fundamentals of Inkjet Printing. Weinheim, Germany: Wiley-VCH; 2016.
50. Hang J, Shi L, Feng X, Xiao L. Electrostatic and electrosteric stabilization of aqueous suspensions of barite nanoparticles. Powder Technol. 2009; 192(2):166-70. https://doi.org/10.1016/j.powtec.2008.12.010.
51. Jenkins P, Snowden M. Depletion flocculation in colloidal dispersions. Adv Colloid Interface Sci. 1996; 6857-96. https://doi.org/10.1016/S0001-8686(96)90046-9.
52. Tuinier R, Introduction to depletion interaction and colloidal phase behaviour. In: Lang P, Liu Y. (eds.) Soft Matter at Aqueous Interfaces. Cham, Switzerland: Springer International Publishing; 2016.
53. Pu Z, Fan X, Su J, Zhu M, Jiang Z. Aqueous dispersing mechanism study of nonionic polymeric dispersant for organic pigments. Colloid Polym. Sci. 2022; 300(3):167-76. https://doi.org/10.1007/s00396-021-04937-z.

How to cite this article:
Jalili M, Mohammad Raei Naeini M, Bastani S, Ajili N. Optimizing the Surfactant/Polymeric Dispersant Combination in Pigment-Based Aqueous Inkjet Inks. Prog Color Colorants Coat. 2025;18(2):177-188. https://doi.org/ 10.30509/pccc.2024.167361.1316.